

Acoustic backscattering measurement from sandy seafloor at 6–24 kHz in the South Yellow Sea

Guangming Kan^{1,2}, Baohua Liu^{2,3*}, Zhiguo Yang^{2,3}, Shengqi Yu^{2,3}, Lehua Qi^{1,4}, Kaiben Yu^{2,3}, Yanliang Pei^{1,2}

¹ Key Laboratory of Marine Sedimentology and Environmental Geology, First Institute of Oceanography, Ministry of Natural Resources, Qingdao 266061, China

² Laboratory for Marine Geology and Environment, Pilot National Laboratory for Marine Science and Technology (Qingdao), Qingdao 266237, China

³ National Deep Sea Center, Ministry of Natural Resources, Qingdao 266237, China

⁴ College of Marine Geosciences, Ocean University of China, Qingdao 266100, China

Received 6 August 2018; accepted 25 September 2018

© Chinese Society for Oceanography and Springer-Verlag GmbH Germany, part of Springer Nature 2019

Abstract

The acoustic bottom backscattering strength was measured at the frequency range of 6–24 kHz on a typical sandy bottom in the South Yellow Sea by using omnidirectional sources and omnidirectional receiving hydrophones. In the experiment, by avoiding disturbances due to scattering off the sea surface and satisfying the far-field condition, we obtained values of acoustic bottom backscattering strength ranging from –41.1 to –24.4 dB within a grazing angle range of 18°–80°. In the effective range of grazing angles, the acoustic scattering strength generally increases with an increase in the grazing angles, but trends of the variation were distinct in different ranges of frequency, which reflect different scattering mechanisms. The frequency dependence of bottom backscattering strength is generally characterized by a positive correlation in the entire frequency range of 6–24 kHz at the grazing angles of 20°, 40° and 60° with the linear regression slopes of 0.222 9 dB/kHz, 0.513 0 dB/kHz and 0.174 6 dB/kHz, respectively. At the largest grazing angle of 80°, the acoustic backscattering strength exhibits no evident frequency dependence.

Key words: acoustic backscattering strength, sandy bottom, South Yellow Sea, grazing angle dependence, frequency dependence

Citation: Kan Guangming, Liu Baohua, Yang Zhiguo, Yu Shengqi, Qi Lehua, Yu Kaiben, Pei Yanliang. 2019. Acoustic backscattering measurement from sandy seafloor at 6–24 kHz in the South Yellow Sea. *Acta Oceanologica Sinica*, 38(5): 99–108, doi: 10.1007/s13131-019-1388-4

1 Introduction

The ocean bottom is an important boundary for the underwater sound field and the acoustic properties of ocean bottom are important factors that influence the spatial structure of underwater sound field as well as the propagation of sound waves in the sea. The complexity of sound propagation in shallow water at sea is mainly due to the strong interaction between sound waves and the bottom. Without knowing the acoustic properties of the ocean bottom, it is difficult to fully understand the laws of acoustic propagation in oceans. Therefore, it is important for underwater acousticians to measure and study the acoustic properties of the ocean bottom, which is usually treated as a black box (Zou et al., 2014; Zhang et al., 2013; Wen et al., 2006).

When an acoustic wave is incident onto the ocean bottom, it is scattered by the rough interface of the seabed. The scattered waves deviate from the direction of specular reflection and decentralize the wave energy distribution in the seawater, complicating the structure of the underwater sound field. Moreover, reverberation caused by bottom scattering is an important source of ocean reverberation, which is a key factor affecting the per-

formance of underwater sonar and the accuracy of underwater target detection (Peng et al., 2004; Jin et al., 1987; Hu, 2009; Dong et al., 2013). Therefore, studying the properties of acoustic bottom scattering has important applications to the prediction of ocean reverberation, object detection on the ocean bottom, and research on ocean acoustics in general (Gao, 2013; Li and Sun, 2008).

Researchers have conducted numerous measurements and research on acoustic bottom scattering at frequencies higher than 20 kHz (Jackson et al., 1986; Stanic et al., 1988a, b, 1989; Williams et al., 2002, 2009; Williams, 2009). The mid-to-low-frequency acoustic bottom scattering at frequencies lower than 20 kHz (especially lower than 10 kHz) is easily influenced by reflection and scattering from the sea surface, thus making it more challenging to measure and rendering its scattering mechanism more complicated, in comparison with high-frequency acoustic scattering. Researchers have thus begun attending to pay increasing attention to the measurement and research of mid- to low-frequency acoustic bottom scattering. Soukup and Gragg (2003) measured acoustic bottom backscattering at frequencies

Foundation item: The Opening Fund of Pilot National Laboratory for Marine Science and Technology (Qingdao) under contract No. QNLM2016ORP0209; the National Natural Science Foundation of China under contract Nos 41330965, 41676055 and 41527809; the Taishan Scholar Project Funding under contract No. tspd20161007.

*Corresponding author, E-mail: bhliu@ndsc.org.cn

of 2–3.5 kHz on a limestone bottom in the sea area near South Carolina, USA (Soukup and Gragg, 2003). Hines et al. (2005) measured acoustic bottom backscattering at frequencies of 4 and 8 kHz at two sandy bottom sites using parametric array sources with a grazing angle range of 3°–15° (Hines et al., 2005). La and Choi (2010) measured acoustic bottom scattering at a frequency of 8 kHz on a nearshore silty bottom in the southern part of South Korea with a grazing angle range of 6°–31° using omnidirectional sources and omnidirectional hydrophones (La and Choi, 2010). Yu et al. (2017) established a backscattering model for a stratified seafloor applying to low frequency from 0.1 to 10 kHz (Yu et al., 2017). The researches mentioned-above indicate that the acoustic bottom scattering strength is distinct at different frequency range. Beside the frequency dependence of acoustic bottom scattering strength, it also has obvious contrasts for different sediment types (McKinney and Anderson, 1964; Jackson et al., 1986; Stanic et al., 1988a, b, 1989; Jackson and Briggs, 1992; Pouliquen and Lyons, 2002; La and Choi, 2010; Hines et al., 2005). The result from McKinney and Anderson indicates that the acoustic backscattering strength from medium sandy bottom is about 5 dB higher than very fine sandy muddy bottom, but is about 7 dB lower than medium sandy clay bottom at the same grazing angles. The bottom scattering from medium sandy bottom measured by Hines et al. (2005) is about 9 dB higher than that from silty bottom measured by La and Choi (2010). In addition, the acoustic bottom scattering strength is related to the roughness of bottom and the volume heterogeneity in sediments (Jackson and Briggs, 1992; Jackson and Richardson, 2007). Therefore, it is necessary to systematically investigate the acoustic bottom scattering property in a specified area and at a wide frequency range.

At present, the measurement and research of the mid-frequency bottom scattering are only concentrated on several discrete frequency points, rather than continuous and systematic measurement in a wide frequency band. Moreover, current measurements were made in different types of seafloors, which makes difficult to compare the data at different frequencies. This paper reports the procedure and results of an experiment to measure acoustic bottom backscattering at a mid-frequency range of 6–24 kHz on a typical sandy bottom in the South Yellow Sea. Following the introduction, relationships between the characteristics of mid-frequency acoustic backscattering from the sandy bottom and the grazing angle, frequency, and features of bottom sediment are discussed.

2 Measurement of bottom backscattering and data processing

2.1 Measurement of the environmental parameters at seafloor

The study area is located in a sandy bottom region of the South Yellow Sea with the latitude ranging from 34.87°N to 35.37°N and the longitude ranging from 121.01°E to 121.62°E, approximately 70 nautical miles southeast of Qingdao City. At a depth of 36–41 m, the bottom of the study area is flat and the sediment is dominated by fine sand. Three measuring sites were arranged—S1, S2 and S3—in the study area, with depths of approximately 36 m at Sites S2 and S3, and that of approximately 41 m at Site S1. Results of measurement of the sound speed profile of seawater in the area revealed a thermocline approximately 20 m deep in September, with a difference of approximately 20 m/s in the sound speed above and below the thermocline (Fig. 1). Some sediment samples were collected using a box corer. However, as all zones near the three measuring sites had “very hard sand sheet” bottoms, only a small amount of sediment was obtained. Sediments approximately 10 cm thick were obtained at S1 and

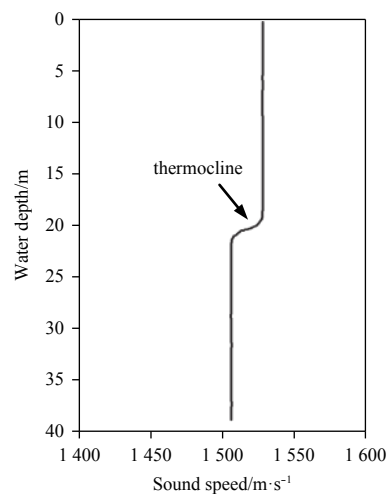


Fig. 1. Sound speed profile in seawater measured in September at Site S1.

S3. The upper 5 cm of the sediments consisted of relatively evenly distributed fine sand and the lower 5 cm had many shell fragments. Photographs of the bottom obtained using an underwater camera show that there are many shell fragment in the bottom at S1 and S3 (Fig. 2). The sampling depth at S2 was approximately 7 cm, where the sediment consists of evenly distributed fine sand without shell fragments (Fig. 2). Results of the measurement of physical properties of the sediment samples show that the content of fine sand in the samples collected at S1 is 79.9%, and the average grain size is in the range from 3.07Φ to 3.35Φ. The content of fine sand in the samples collected at S2 is 86.8%, and the average grain size is in the range from 2.75Φ to 3.04Φ (with an average value of 2.989Φ). The content of fine sand in the samples collected at S3 is 78.4%, and the average grain size is in the range from 2.82Φ to 4.31Φ.

2.2 Method of bottom backscattering strength calculation

The method to measure acoustic bottom backscattering strength by using a spherical omnidirectional source and an omnidirectional hydrophone is shown in Fig. 3. Sound waves transmitted by the acoustic source reach the bottom at Point A at time t (corresponding to a grazing angle of θ), and the backscattered waves from the bottom are received by the hydrophone fixed just below the acoustic source. As the hydrophone is close to the source, the bottom backscattering is regarded as having approximately a monostatic geometry in the experiment. For monostatic bottom backscattering, the ensonified zone at time t is an annulus, and its width is determined by the pulse length of the emitting signal. The slant range from the acoustic source to the inner and outer boundary of the scattering zone is denoted by r and r' , respectively, and is calculated by:

$$r = c_w t / 2, \quad (1)$$

and

$$r' - r = \tau / 2c_w. \quad (2)$$

If the height of the source and hydrophone above the seafloor is denoted by H , the following relationship is obtained according to the geometry in Fig. 3.

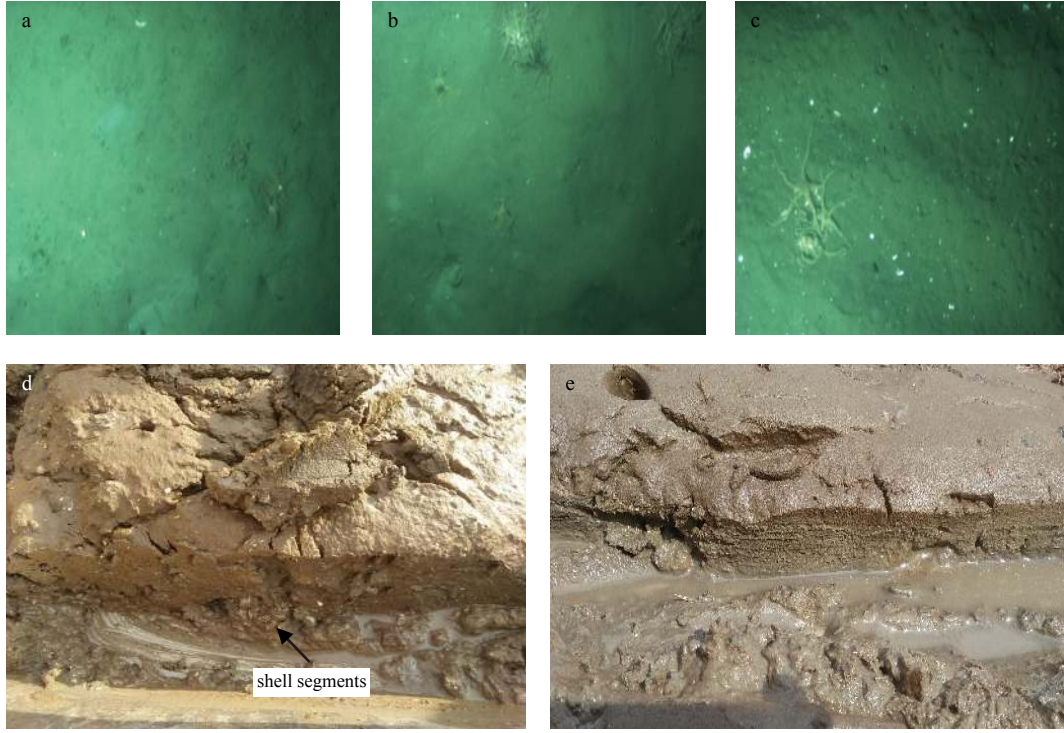


Fig. 2. Photos of bottom obtained using underwater camera and sediment collected using sampling box. a. Bottom photo at S1, b. bottom photo at S2, c. bottom photo at S3, d. sediment collected at S1, and e. sediment collected at S2.

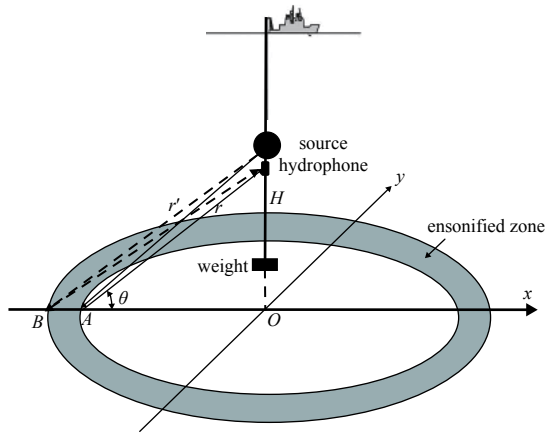


Fig. 3. Diagram of backscattering measurement using an omnidirectional source and an omnidirectional hydrophone.

$$r^2 = H^2 + R^2, \quad (3)$$

and

$$r'^2 = H^2 + R'^2, \quad (4)$$

where R and R' are the distance from Point O to Points A and B , respectively. The area of the ensonified zone on the bottom can then be calculated as

$$A = \pi (R'^2 - R^2). \quad (5)$$

Combining Eqs (1)–(5), we get:

$$A = \pi \left(r + \frac{1}{4} c_w \tau \right) c_w \tau, \quad (6)$$

where τ is the length of the transmitted signal, c_w is the sound speed in seawater, and θ is the grazing angle.

For bottom backscattering using an omnidirectional source and an omnidirectional hydrophone in case both are (or approximately are) at the same position, the intensity of the scattered sound corresponding to grazing angle θ can be expressed as

$$\langle I_s(\theta) \rangle = \int \frac{I_0}{r^4} \sigma(\theta) dA, \quad (7)$$

where $I_s(\theta)$ is the scattering intensity at grazing angle θ , and the angle bracket “ $\langle \rangle$ ” denotes the average value of the random variable over the entire measurement set accounting for the randomness of the scattering intensity. In measurement in practice, random samples are typically obtained by transmitting the sound many times from a survey ship floating near the site. I_0 is the intensity of the incident sound one meter from the acoustic source, $\sigma(\theta)$ is the backscattering cross section, r is the slant range from the acoustic source to the inner boundary of the scattering zone corresponding to a grazing angle θ , and dA is the differential element of the area of the ensonified zone on the bottom.

Equation (7) can be rewritten in terms of the real voltage output of the hydrophone as (under the condition that the change in r over Area A is small enough)

$$\langle v_r(t)^2 \rangle = \frac{s_t^2 s_r^2}{r^4} \int \sigma(\theta) dA, \quad (8)$$

where $v_r(t)^2$ denotes the mean square value of the real voltage output of the hydrophone in volt before being amplified. Parameters s_t and s_r are related to the source level and the sensitivity

of the hydrophone, respectively, as

$$SL = 20 \log_{10}(s_t/10^{-6}), \quad (9)$$

$$RS = 20 \log_{10}(s_r/10^6), \quad (10)$$

where SL is the acoustic source level of the acoustic source in dB *re.* 1 μPa one meter from the source, and RS is the sensitivity of hydrophone in dB *re.* 1 $\text{V}/\mu\text{Pa}$. SL and RL can be measured through the calibration of the source and the hydrophone, respectively, in the laboratory. If the change in grazing angle θ is small enough such that $\sigma(\theta)$ is approximately constant over the ensonified zone, the bottom backscattering strength can be calculated by the following sonar equation,

$$S_b(\theta) = 10 \log_{10} \sigma(\theta) = 10 \log_{10} \langle v_r(t)^2 \rangle - SL - RS + 2TL - 10 \log_{10}(A), \quad (11)$$

where $S_b(\theta)$ is the backscattering strength at grazing angle θ in dB, $TL=20 \log_{10} r$ is the one-way transmission loss in dB, and A is the area of the ensonified zone shown in Fig. 3, $v_r(t)$ is the output of the effective voltage from the hydrophone and can be approximately expressed by the envelope $V_r(t)^2$ as

$$v_r(t)^2 = \frac{V_r(t)^2}{2}. \quad (12)$$

In Eq. (11), TL and A are related to the slant range r , which is represented in terms of θ as

$$r = H/\sin\theta. \quad (13)$$

According to different grazing angle θ , the slant range r can be calculated by Eq. (13). Then, TL and A can be obtained. Finally, the acoustic bottom backscattering strength $S_b(\theta)$ can be calculated by using Eqs (11) and (12).

2.3 Description of the experiment and data processing

In this experiment, three spherical omnidirectional source transducers with central frequencies of 8 kHz, 15 kHz and 20 kHz, respectively, and an omnidirectional broadband hydrophone were used to measure the acoustic bottom backscattering strength. The geometry of the experiment is shown in Fig. 4. A TL-30 hydrophone was located one meter below the spherical acoustic sources and was connected to a single-channel self-contained recorder that had an acoustic wave sampling rate of 96 kHz. The sound waves received by the TL-30 hydrophone were used to calculate the bottom backscattering strength. Moreover, an HTI hydrophone on one side of the source, connected to a real-time recorder in a deck laboratory, was used to monitor the acoustic waves emitted by the source. The spherical acoustic sources were generally 7–8 m from the bottom. Self-contained temperature and depth (short for STD) recorders were fixed near the acoustic source and the hydrophone to monitor the distances between each and the bottom. The acoustic source levels of the three spherical transducers at their central frequencies were 203 dB *re.* 1 μPa at 8 kHz, 201 dB *re.* 1 μPa at 15 kHz, and 205 dB *re.* 1 μPa at 20 kHz. The sensitivity of the TL-30 omnidirectional broadband hydrophone in an operating band of 2.5–60 kHz was -197 to -190 dB *re.* 1 $\text{V}/\mu\text{Pa}$. During the experiment, the survey ship floated near the corresponding measure-

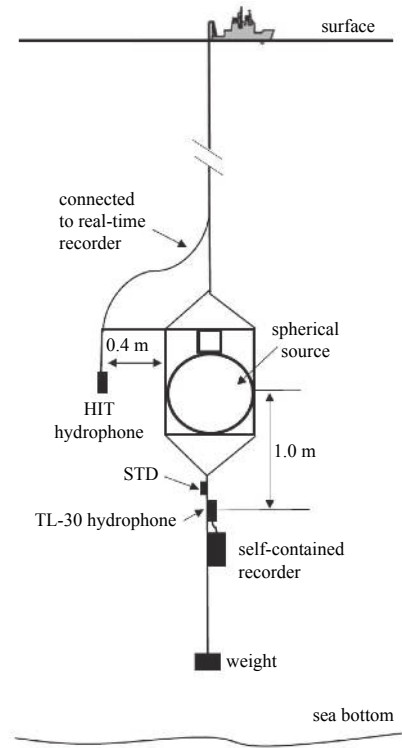


Fig. 4. The geometry of the bottom backscattering measurement.

ment site, transmitting a 1 ms sinusoidal pulse signal every time and repeating the signal 90 times at an interval of 2 s. In the range 6–24 kHz, the above operation was repeated at a frequency interval of 1 kHz so that the signal could cover all frequencies.

According to the maximum effective recording length and transmitting interval, the waveform of each ping at the target frequency was extracted from the entire data set. The received original signals with 90 waveforms superposed at frequencies of 8 kHz and 22 kHz are shown in Fig. 5. The first arrival waveform, the bottom reflected waveform, and the sea surface reflected waveform can be clearly identified in the figure. Because the hydrophone is very close to the acoustic source, the amplitude of the first arrival waveform is beyond the dynamic range of the acquisition unit, and resulted in signal truncation. The weak scattered signal after the first arrival wave (at 4–5 ms) is the acoustic scattering from the weight. By comparing Fig. 5a with Fig. 5b, it is evident that with an increase in frequency, acoustic scattering from the weight becomes more prominent. The zone after the bottom-reflected signal (~ 10 ms) is the acoustic bottom scattering zone. The signal after 39 ms can not be used to calculate bottom scattering due to the influence of reflection and scattering from the sea surface. The signal that can be used to calculate the acoustic bottom scattering strength is limited between the bottom-reflected signal and the sea surface-scattered signal, and determines the range of the grazing angle for the calculation of the bottom backscattering strength. In shallow sea, due to the influence of reflection and scattering from the sea surface, the scattering strength can not be calculated when the grazing angle is very small, which is a shortcoming of measuring bottom scattering using an omnidirectional source and an omnidirectional hydrophone. According to the characteristics of the signal shown in Fig. 5 and the corresponding measurement geometry, the calculated lower limit of the grazing angle to measure scattering strength is approximately 18° . In this experiment, distances from

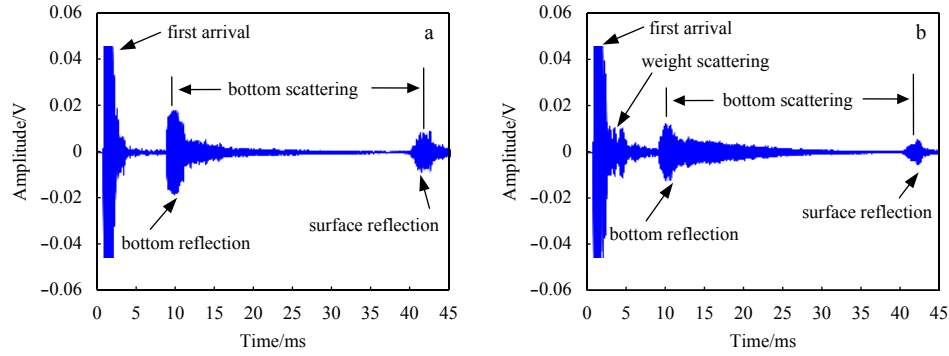


Fig. 5. Waveform received by TL-30 hydrophone at Site S1. a. 8 kHz, and b. 22 kHz.

both the acoustic source and the hydrophone to the bottom are greater than 5 m, thus satisfying the far-field conditions. Therefore, the upper limit of the grazing angle is mainly determined by the characteristics of the bottom reflected and scattered signals, and it was set to 80° in this experiment.

At first, the amplitude envelope of the temporal waveform of each ping, i.e., the voltage value output from the hydrophone $V(t)$, was obtained through a Hilbert transform of temporal series of the waveform at one target frequency. Generally, the mean value of amplitude envelope for different pings at the same target frequency was used to calculate the scattering strength in order to eliminate the random noise. Then, the amplitude envelopes were calculated at all frequencies from 6 kHz to 24 kHz with 1 kHz step. As an example, the amplitude envelopes of 90 effective pings at two frequencies of 8 kHz and 22 kHz were superposed and drawn in Fig. 6 corresponding the waveform in Fig. 5. Their averaged envelopes of 90 effective pings were also shown in Fig. 6 with red curves. The procedure of scattering strength calculation was as follows. Firstly, at one target frequency, the grazing angle θ ranges from 18° to 80° with the step of 1° . According to Eq. (13) and Eq. (6), the slant range r and the area of the ensonified zone A corresponding to each grazing angle θ are calculated. Secondly, The effective voltage value $v_r(t)$ corresponding to each grazing angle θ and slant range r was calculated by using Eq. (12), where the $V(t)$ in Eq. (12) was averaged over 90 pings and t can be obtained by using $t = 2r/c_w$. The one-way transmission loss can be calculated according to the formula of $TL = 20 \log_{10} r$. Finally, By substituting the effective voltage value $v_r(t)$, the one-way transmission loss TL , the area of the ensonified zone A into Eq. (11), the acoustic bottom backscattering strength $S_b(\theta)$ at one target frequency can be obtained with the grazing angle ranging from

18° – 80° , where SL and RS can be obtained through the calibration of source level of omni-directional source and receiving sensitivity of omni-directional hydrophone. The bottom backscattering strength at frequencies in the range of 6–24 kHz can be calculated by repeating the three processes for each target frequency when the frequency ranges from 6 kHz to 24 kHz with the step of 1 kHz. The calculation results show that the acoustic bottom scattering strength falls between -41.1 and -24.4 dB in the grazing angle range of 18° – 80° and in the frequency range of 6–24 kHz.

3 Results and discussion

3.1 Relationship between the backscattering strength and the grazing angle

Figure 7 shows the relationship between the acoustic bottom scattering strength and the grazing angles at different frequencies in S1. It is clear that the range of the effective grazing angle is 18° – 80° in this experiment, over which the acoustic bottom scattering strength was obtained effectively. Due to the influence of sea surface reflection, the scattering strength at smaller grazing angles could not be calculated correctly, which is a limitation in measuring acoustic scattering in shallow water using omnidirectional sources and receivers. Figure 7 shows that the acoustic bottom scattering strength at S1 generally increases with an increase in the grazing angle, but the trends of variation are different at different frequencies. In different frequency bands and at different grazing angles, the acoustic scattering strength exhibits different properties. In the frequency band 6–18 kHz, the scattering strength increases rapidly with the grazing angle for angles greater than 70° , which is the so-called backscattering enhance-

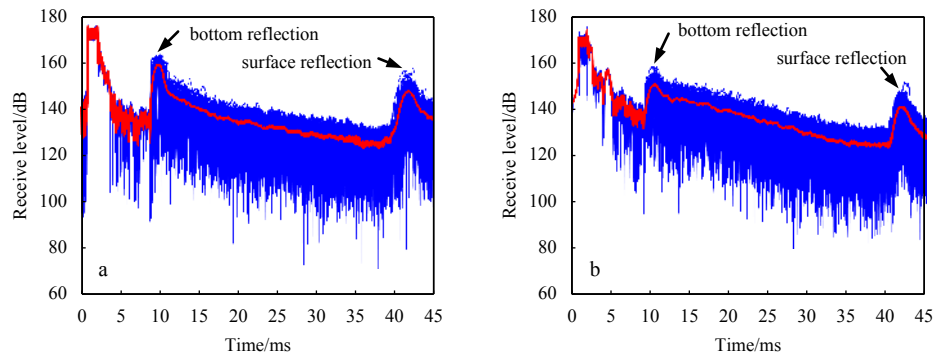


Fig. 6. Envelopes corresponding to the waveform in Fig. 5. Blue curves are envelopes for 90 realization and red curve is their averaged envelope. a. 8 kHz, and b. 22 kHz.

ment phenomenon. This indicates that acoustic scattering for grazing angles greater than 70° is not completely diffuse, but is significantly enhanced along the direction near to the specular reflection. In the frequency band 20–24 kHz, there is no signif-

icant enhancement in backscattering for grazing angles greater than 70° . With an increase in frequency, the trend of variation in scattering strength with grazing angle tends to be gentle at large grazing angles. In particular at 24 kHz, the scattering strength ex-

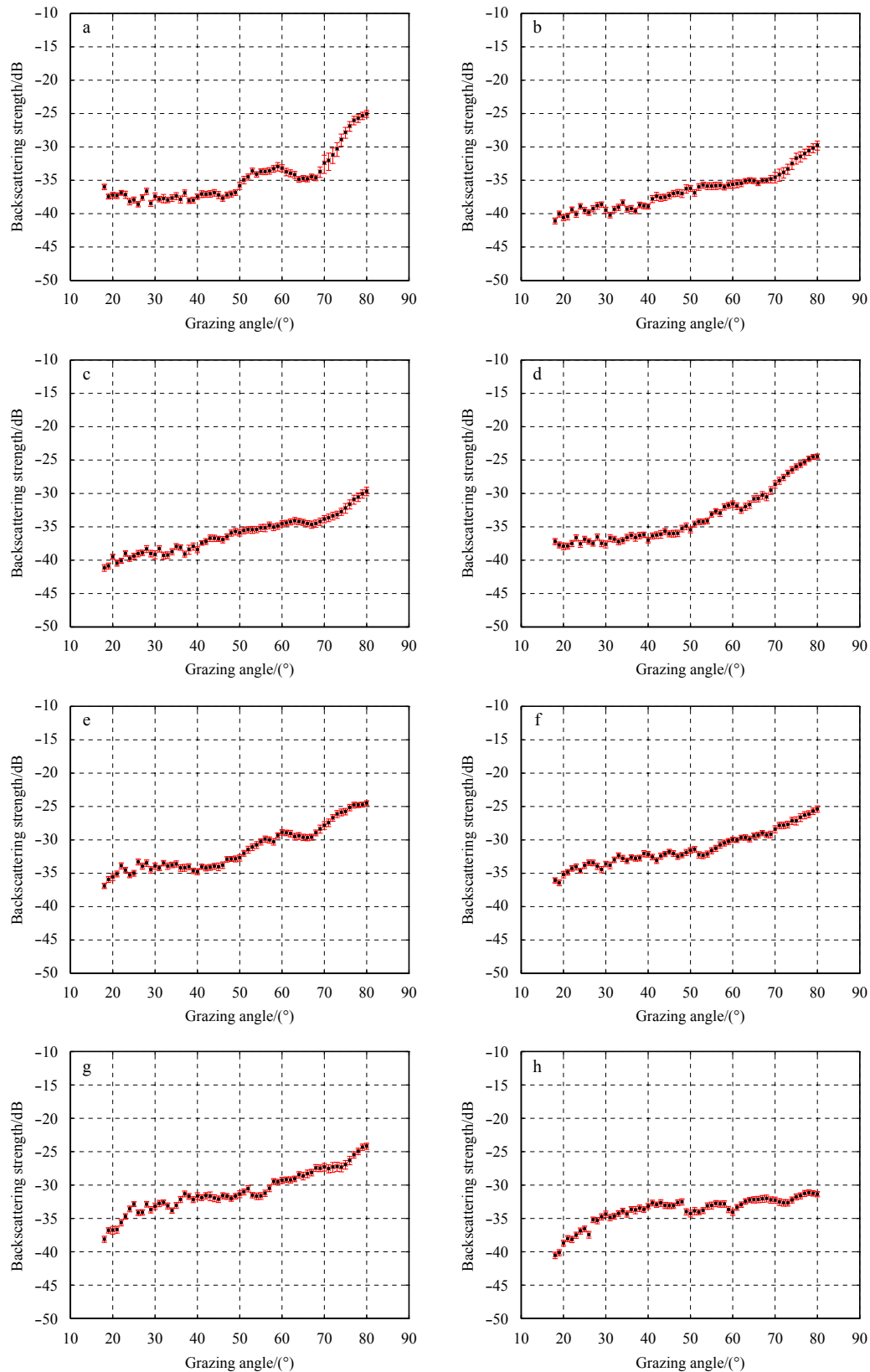


Fig. 7.

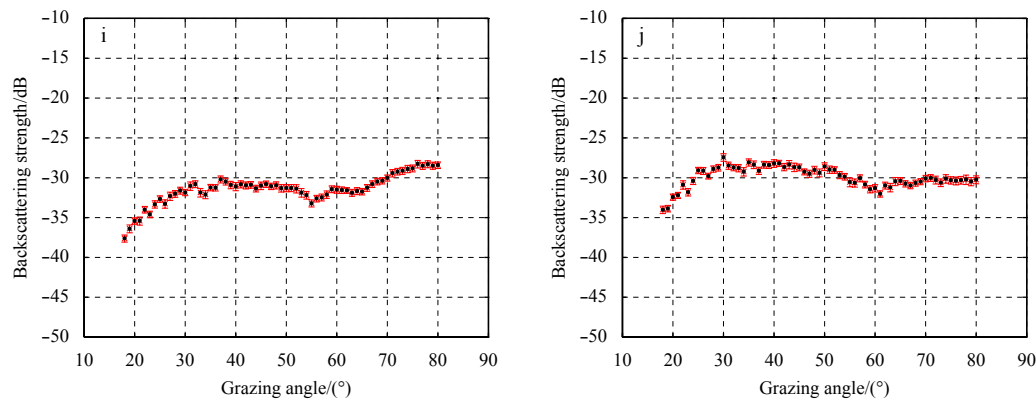


Fig. 7. Relationships between the backscattering strength and the grazing angles at different frequencies at Site S1. a. 6 kHz, b. 8 kHz, c. 10 kHz, d. 12 kHz, e. 14 kHz, f. 16 kHz, g. 18 kHz, h. 20 kHz, i. 22 kHz, and j. 24 kHz.

hibit a decrease with an increase in the grazing angles greater than 50° , perhaps because of the low SNR (signal-to-noise ratio) at high frequency. The different trends of variation in scattering strength with grazing angle at different frequency bands reflect different acoustic scattering mechanisms, and this needs to be analyzed comprehensively combining with such bottom environmental parameters as bottom roughness and geoacoustic properties.

Hines et al. (2005) conducted measurements using parametric array sources at two well-sorted medium sandy bottom sites with the grain sizes ranging from 1.39Φ to 0.69Φ (0.25–0.50 mm) in the New Jersey continental shelf area and the Scotian continental shelf area, and obtained acoustic bottom backscattering strength values of -25.4 to -23.1 dB, and of -29.0 to -26.1 dB, respectively, at a grazing angle of 15° and a frequency of 8 kHz (Hines et al., 2005). Figure 7b shows that the backscattering strength varies from -41.1 to -40.6 dB at S1 at the grazing angles ranging from 18° to 20° and a frequency of 8 kHz, lower than the results measured by Hines et al. (2005). La and Choi (2010) conducted measurements on a nearshore silty bottom in South Korea to obtain bottom backscattering strength of approximately -33 dB within a grazing angle range of 18° – 20° and at a frequency of 8 kHz, which is approximately 8 dB higher than the backscattering strength at Site S1 (La and Choi, 2010). Bottom backscattering strength measured by Jackson et al. (1986) at a site with very fine sand bottom and grain size of 0.12 mm is approximately -24 dB at a grazing angle of 20° at 20 kHz. This is approximately 16 dB higher than the results obtained in our experiment at the same grazing angle (20°) and frequency (20 kHz) (Jackson et al., 1986), where the grain sizes are very similar. Jackson et al. (1986) pointed out that scattering strength can differ by 10–15 dB for sediments with similar grain size. This difference indicates that the mechanism of acoustic bottom scattering is very complex and is dominated not only by grain size, but also by the roughness of the bottom, heterogeneity of the sediment and other factors.

3.2 Frequency dependence of the backscattering strength

For the dependence of the acoustic bottom backscattering strength on acoustic wave frequency, different researchers have calimed different relationships according to different bottom types and measurement frequencies. The data collected by Jackson et al. (1986) in Puget Sound exhibited a frequency dependence with a positive slope of 1.4 dB/octave at a frequency of 20–85 kHz and a grazing angle of 20° for a silty sand bottom and a frequency dependence with a positive slope of 0.8 dB/octave at a frequency of 20–80 kHz and a grazing angle of 20° for a very fine

sand bottom. However, another set of data obtained by Jackson at a North Sea site exhibited a frequency dependence with a negative slope of -0.2 dB/octave at a frequency of 20–75 kHz and a grazing angle of 20° for sandy silt bottom (Jackson et al., 1986). Based on the results measured on the nearshore shell-rich coarse sand bottom in Jacksonville, Florida, Stanic et al. (1989) found that acoustic bottom backscattering strength exhibited a negative correlation with frequency with a slope of -0.75 dB/octave in the frequency range of 20–180 kHz (Stanic et al., 1989). At present, few studies have addressed the frequency dependence of acoustic bottom backscattering in the mid-frequency band of 6–24 kHz. Figure 8 shows the curves of variation in backscattering strength with grazing angle at different frequency ranges based on the results in this experiment. It is evident from Fig. 8a that the frequency dependence of backscattering strength is very weak and there is no clear trend in the variation of the backscattering strength with frequency at 6–12 kHz. The scattering strength shows a relatively significant frequency dependence in the range from 12 kHz to 24 kHz, as shown in the Figs 8b and c, where the backscattering strength increases with an increase in frequency except at grazing angles greater than 65° . Four grazing angles (i.e., 20° , 40° , 60° , 80°) were chosen to draw the curves of backscattering strength versus frequency, as shown in Fig. 9. It shows that the frequency dependence of acoustic backscattering strength can be generally characterized by a positive correlation with frequency as a whole in the range of 6–24 kHz. As listed in Table 1, the slopes of linear regression between backscattering strength and the frequency in the range of 6–24 kHz at grazing angles of 20° , 40° and 60° are 0.222 9 dB/kHz, 0.513 0 dB/kHz and 0.174 6 dB/kHz, respectively. The result of measurements of the environmental parameters on the bottom indicates that the bottom at Site S1 is very flat, and has no significant local relief such as sand ripples on the bottom. Therefore, the bottom backscattering is mainly caused by the micro-roughness of the bottom and is more sensitive for higher frequency, which corresponds to the frequency dependence of backscattering strength whereby the latter increases with the former. The backscattering strength shows no evident frequency dependence at 80° , perhaps because of the inclusion of some coherent component in backscattering field and the poor quality data at the largest grazing angle of 80° .

3.3 Relationship between the backscattering strength and the bottom sediment properties

Figure 10 shows a comparison of backscattering strength among Sites S1, S2 and S3 at a frequency of 11 kHz. It is evident

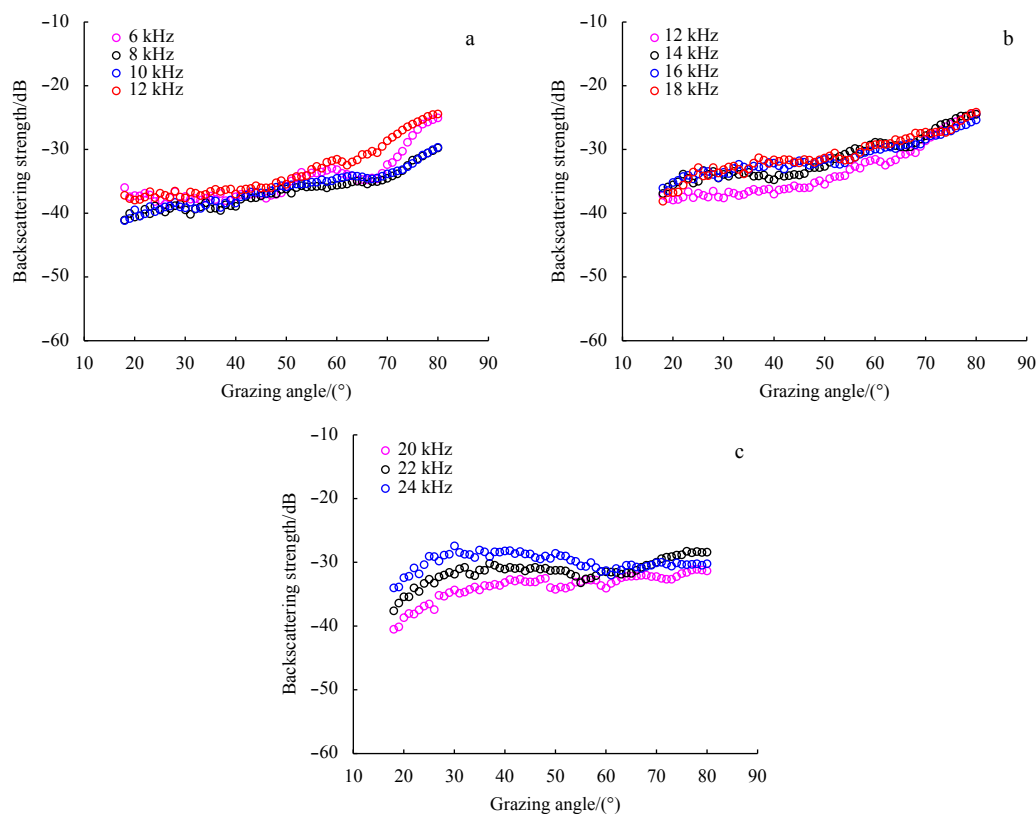


Fig. 8. Relationship between backscattering strength and frequency at different grazing angles at Site S1. a. 6–12 kHz, b. 12–18 kHz, c. 20–24 kHz.

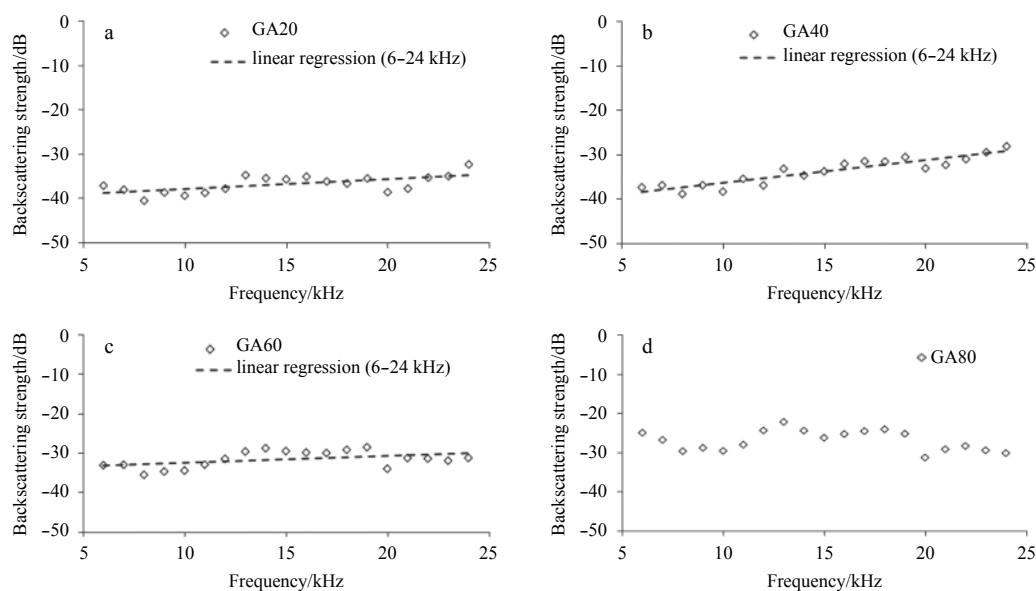


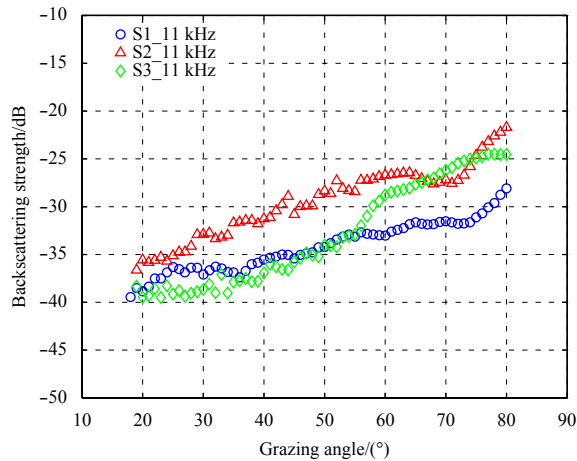
Fig. 9. Frequency dependence of backscattering strength at frequency ranges of 6–24 kHz at different grazing angles at Site S1. Grazing angle: a. 20°, b. 40°, c. 60°, and d. 80°.

that the backscattering strength at S2 is significantly higher than that at S1. The maximum and minimum offsets are 7.03 dB and 1.18 dB, respectively, and the average is 4.63 dB. The corresponding grazing angles for the maximum and minimum offsets are 78° and 25°, respectively. The backscattering strength at S2 is higher than that at S3 as a whole, excepting in the grazing angle from 67° to 73°. The the maximum offset is 7.8 dB at the grazing angle of

74°. The results of measurements of the physical properties of the bottom sediment show that the sediments at S2 have larger grain size and higher content of sandy grain than at S1 and S3. The difference in grain size of bottom sediments among the three sites might be the main cause of the above difference in backscattering strength. In addition, as shown in Fig. 2, there are a large number of shell fragments in the sediment at Sites S1 and S3, but

Table 1. Parameters of linear regression between backscattering strength and frequency at 6–24 kHz at Site S1

Grazing angle/(°)	Equation of linear regression	Slope/dB·kHz ⁻¹	Correlation coefficient
20	BBS=0.222 9×f-40.207	0.222 9	0.63
40	BBS=0.513 0×f-41.552	0.513 0	0.92
60	BBS=0.174 6×f-34.303	0.174 6	0.46

**Fig. 10.** Comparison of backscattering strength among Sites S1, S2 and S3.

no evident shell fragments in that at Site S2. The presence of shell fragment in the sediment might be another factor contributing to the difference of backscattering strength. Shell fragments in the sediment cause diffuse scattering of the sound waves along all directions, resulting in a reduction in along the direction of the backscattering.

4 Conclusions

(1) By avoiding disturbance from scattering off the sea surface and satisfying the far-field condition, we successfully measured the acoustic bottom backscattering strength, which ranges from -41.1 to -24.4 dB in a grazing angle range of 18°–80° and a frequency range of 6–24 kHz. Within the range of the effective grazing angle, the acoustic scattering strength generally increases with an increase in grazing angles, but the trends of the variation are different at different frequencies, which reflect different scattering mechanisms. Because of the very shallow water depth in the study area (only approximately 40 m in deep), the scattering strength at grazing angles lower than 18° can not be obtained in this experiment by using the omnidirectional source and receiver. In order to obtain bottom backscattering strength at lower grazing angle, more advanced instruments such as parametric array source with directional beam and vertical array with many receiving elements are needed.

(2) The frequency dependence of the bottom backscattering strength is generally characterized by a positive correlation in the entire frequency range of 6–24 kHz at the grazing angles of 20°, 40° and 60° with the linear regression slopes of 0.222 9 dB/kHz, 0.513 0 dB/kHz, and 0.174 6 dB/kHz, respectively. At a grazing angle of 80°, the acoustic backscattering strength exhibits no evident frequency dependence in the range of 6–24 kHz. The probable reasons lie in the inclusion of some coherent component in backscattering field and the poor quality data at the largest grazing angle.

(3) The acoustic scattering strength varies with the properties of the bottom sediment. The backscattering strength from the

bottom with larger grain size and shell-free sediment is approximately 1–8 dB higher than that from a bottom with smaller grain size and shell-rich sediment. The difference in grain size of bottom sediment and the presence of shell segments in it may be important factors that lead to this difference in the backscattering strength at S1, S2 and S3.

Acknowledgments

We gratefully acknowledge all our colleagues and the crews of the R/V *Xiangyanghong* 81 for their assistance with the collection of data.

References

- Dong Zhongchen, Li Yanan, Jin Yanfeng. 2013. Shallow seafloor reverberation modeling and simulation of torpedo. *Torpedo Technology* (in Chinese), 21(2): 100–104
- Gao Bo. 2013. Modeling and characteristic of long-range bottom reverberation in shallow water (in Chinese) [dissertation]. Harbin: Harbin Engineering University
- Hines P C, Osler J C, MacDougald D J. 2005. Acoustic backscatter measurements from littoral seabeds at shallow grazing angles at 4 and 8 kHz. *The Journal of the Acoustical Society of America*, 117(6): 3504–3516, doi: [10.1121/1.1898064](https://doi.org/10.1121/1.1898064)
- Hu Jianzhong. 2009. Measurement and model calculation of sea bottom three-dimensional scattering strength (in Chinese) [dissertation]. Harbin: Harbin Engineering University
- Jackson D R, Baird A M, Crisp J J, et al. 1986. High-frequency bottom backscatter measurements in shallow water. *The Journal of the Acoustical Society of America*, 80(4): 1188–1199, doi: [10.1121/1.393809](https://doi.org/10.1121/1.393809)
- Jackson D R, Briggs K B. 1992. High-frequency bottom backscattering: roughness versus sediment volume scattering. *The Journal of the Acoustical Society of America*, 92(2): 962–977, doi: [10.1121/1.403966](https://doi.org/10.1121/1.403966)
- Jackson D R, Richardson M D. 2007. *High-frequency seafloor acoustics*. New York: Springer Science+Business Media, LLC
- Jin Guoliang, Wu Chengyi, Zhang Guohua, et al. 1987. The measurement of two-dimensional bottom backscattering coefficients at shallow water. *Acta Acustica* (in Chinese), 12(3): 227–231
- La H, Choi J W. 2010. 8-kHz bottom backscattering measurements at low grazing angles in shallow water. *The Journal of the Acoustical Society of America*, 127(4): EL160–EL165, doi: [10.1121/1.3338987](https://doi.org/10.1121/1.3338987)
- Li Songwen, Sun Liangyi. 2008. Subcritical detection of buried mine - a review on the theories, experiments and equipment. *Ship Electronic Engineering* (in Chinese), 28(2): 136–140
- McKinney C M, Anderson C D. 1964. Measurements of backscattering of sound from the ocean bottom. *The Journal of the Acoustical Society of America*, 36(1): 158–163, doi: [10.1121/1.1918927](https://doi.org/10.1121/1.1918927)
- Peng Zhaoxun, Zhou Jixun, Zhang Renhe. 2004. In-plane bistatic backward scattering from seabottom with randomly inhomogeneous sediment and rough interface. *Science in China Series G: Physics, Mechanics and Astronomy*, 47(6): 702–716, doi: [10.1007/BF02687341](https://doi.org/10.1007/BF02687341)
- Pouliquen E, Lyons A P. 2002. Backscattering from bioturbated sediments at very high frequency. *IEEE Journal of Oceanic Engineering*, 27(3): 388–402, doi: [10.1109/JOE.2002.1040926](https://doi.org/10.1109/JOE.2002.1040926)
- Soukup R J, Gragg R F. 2003. Backscatter from a limestone seafloor at 2–3.5 kHz: measurements and modeling. *The Journal of the Acoustical Society of America*, 113(5): 2501–2514, doi: [10.1121/1.1558039](https://doi.org/10.1121/1.1558039)

- Stanic S, Briggs K B, Fleischer P, et al. 1988a. Shallow-water high-frequency bottom scattering off Panama City, Florida. *The Journal of the Acoustical Society of America*, 83(6): 2134–2144, doi: [10.1121/1.396341](https://doi.org/10.1121/1.396341)
- Stanic S, Briggs K B, Fleischer P, et al. 1989. High-frequency acoustic backscattering from a coarse shell ocean bottom. *The Journal of the Acoustical Society of America*, 85(1): 125–136, doi: [10.1121/1.397720](https://doi.org/10.1121/1.397720)
- Stanic S, Eckstein B E, Williams R L, et al. 1988b. A high-frequency, shallow-water acoustic measurement system. *IEEE Journal of Oceanic Engineering*, 13(3): 155–162, doi: [10.1109/48.572](https://doi.org/10.1109/48.572)
- Wen Mingming, Xiao Bo, Cui Huayi. 2006. The method for measuring the acoustics characteristic of the ocean sediment. *Ocean Technology (in Chinese)*, 25(1): 124–126
- Williams K L. 2009. Forward scattering from a rippled sand/water interface: modeling, measurements, and determination of the plane wave, flat surface reflection coefficient. *IEEE Journal of Oceanic Engineering*, 34(4): 399–406, doi: [10.1109/JOE.2008.2002121](https://doi.org/10.1109/JOE.2008.2002121)
- Williams K L, Jackson D R, Tang Dajun, et al. 2009. Acoustic backscattering from a sand and a sand/mud environment: experiments and data/model comparisons. *IEEE Journal of Oceanic Engineering*, 34(4): 388–398, doi: [10.1109/JOE.2009.2018335](https://doi.org/10.1109/JOE.2009.2018335)
- Williams K L, Jackson D R, Thorsos E I, et al. 2002. Acoustic backscattering experiments in a well characterized sand sediment: data/model comparisons using sediment fluid and biot models. *IEEE Journal of Oceanic Engineering*, 27(3): 376–387, doi: [10.1109/JOE.2002.1040925](https://doi.org/10.1109/JOE.2002.1040925)
- Yu Shengqi, Liu Baohua, Yu Kaiben, et al. 2017. A backscattering model for a stratified seafloor. *Acta Oceanologica Sinica*, 36(7): 56–65, doi: [10.1007/s13131-017-1084-1](https://doi.org/10.1007/s13131-017-1084-1)
- Zhang Renhe, Li Zhenglin, Peng Zhaohui, et al. 2013. Overview of shallow water acoustics. *Scientia Sinica Physica, Mechanica & Astronomica (in Chinese)*, 43(S1): S2–S15
- Zou Dapeng, Kan Guangming, Long Jianjun. 2014. Methods of in-situ acoustic measurement of seafloor surface sediment. *Haiyang Xuebao (in Chinese)*, 36(11): 111–119